The Application of Airborne Radar Altimetry to the Measurement of Height and Slope of Isobaric Surfaces

E. N. BROWN, M. A. SHAPIRO, P. J. KENNEDY AND C. A. FRIEHE

National Center for Atmospheric Research,[1] Boulder, CO 80307

(Manuscript received 8 January 1981, in final form 6 June 1981)

ABSTRACT

The aeronautical use of electronic altimeters is to measure the absolute clearance of an aircraft above the earth's surface. In the support of atmospheric research, accurate high-range altimeters, in conjunction with accurate static pressure and navigation data, also can provide a means for measuring the heights of constant-pressure surfaces. From the derivatives of the measurements, surface slopes and dynamical quantities such as the geostrophic wind may be obtained. Although the technique is easiest over oceans or large bodies of water, it can be successfully used over land, if detailed terrain heights are known.

This paper describes the operational and research use of a high-altitude pulse-type radar altimeter system installed on the NCAR Sabreliner for jet stream research. An error analysis for "*D*-value", derived from radar altitude and pressure measurements, gave an estimated error of ±6.0 m, which surpasses measurements from conventional balloon soundings or satellite-derived height analyses. For a case study of jet stream dynamics, the above error in *D*-value corresponded to an error of ±5% in the computed geostrophic wind.

1. General description and principle of operation

A high-altitude radar altimeter, such as the APN-159, is designed to provide high reliability and accuracy over the altitude range 0–21 km. The system's specifications are listed in Table 1 and a functional block diagram of the system is shown in Fig. 1. In principle, its operation involves ranging, or measuring the time elapsed between transmitted and received signals (Fig. 2).

The transmitter section of the receiver-transmitter (RT) unit generates periodic pulses of radio frequency (rf) energy, which are delivered to the transmitter antenna on the underside of the aircraft. From this antenna the pulsed energy is radiated downward, reflected at the earth's surface, and returned to the receiver antenna. The time elapsed between transmission and reception of the rf pulse is determined by the absolute altitude of the aircraft above the reflecting surface. The receiver antenna delivers the returned pulse to the receiver section of the RT unit where it is amplified, detected, and shaped for driving a servo shaft assembly which is referenced to an internal pulse coincident with the transmission time. The servo assembly feeds information to the indicator unit for display purpose and provides additional outputs for recording purposes.

A very important feature is the automatic calibration system, which checks a simulated received pulse representing zero altitude. This check of 1 s duration occurs once every 3 min; if the output is different than zero, the system automatically adjusts the timing of the transmitter trigger pulse to restore the correct calibration. This assembly provides a secondary, but important, function of automatically insuring that the altitude-computing circuits are functioning properly.

The built-in test (BIT) assembly enables the operator to make four in-flight checks: go/no-go tests for receiver sensitivity (−80 ± 5 dbm), transmitter frequency (1,630 ± 4 MHz; ±0.24% rated frequency), and transmitter peak power (≥500 W), and an equivalent 1524 m internal test to verify system accuracy.

2. System installation and evaluation

Fig. 2 illustrates the external configuration of the antennas on the NCAR Sabreliner. To simplify structural mounting and reduce installation costs, antennas were installed in unpressurized areas of the aircraft. This limited the choice of locations, but antenna separation of 5.2 m was achieved. The antennas were contained in removable pod assemblies and were fabricated so that the antenna surfaces were horizontal for the nominal Sabreliner pitch angle of +3.5°. Since there were no large external stores on the aircraft undercarriage, the normal radiation pattern of the antenna was not altered. The RT installation in the pressurized cabin provided ideal environmental conditions while minimizing the length of the coaxial cables and the number of connectors to the antennas. The coaxial cables to the receiver and transmitter antennas were of identical length.

[1] The National Center for Atmospheric Research is sponsored by the National Science Foundation.

0021-8952/81/091070-06$05.50

TABLE 1. APN-159 specifications.

Total weight	16 kg
Transmitter-receiver frequency	1630 MHz (nominal), L Band
Transmitter power	1 KW (peak)
Transmitter pulse repetition frequency	4.916 KHz ± 2 Hz
Transmitter pulse width	0.040 μs below 609 m 0.150 μs above 609 m
Attitude function limits	±18° (pitch or roll)
Antenna beam width	45° (E plane) to 55° (H plane)
Altitude tracking rate	152 m s^{-1}
Altitude accuracy (synchro)	±2.4 m or 1%, whichever is greater
Altitude range	0–21 341 m

Auxiliary outputs: The receiver-transmitter servo shaft assembly provides two pair of absolute synchro signals: a coarse synchro with a sensitivity of 30 487 m $(360°)^{-1}$ and a fine synchro of 1219.5 m $(360°)^{-1}$.

The output of the servo assembly comprised two synchro signals of fine and coarse resolution, proportional to altitude (see Table 1). These were converted to digital form with two 14-bit synchro-to-digital converters and were interfaced into the aircraft digital data acquisition system (ARIS IV) through two parallel ports (Duncan and Brown, 1978). The sample rate was 5 Hz. In the final computer analysis, the altitude was reconstructed from the two signals with a final resolution of 0.07 m.

In order to assess the performance of the APN-159 in meteorological research, several tests were performed to ascertain the signal variation, accuracy, and drift of the system. Short-term variation was measured by two methods: calculation of the standard deviation of 1 s mean altitude data from the instrument during a 2 min period of straight and level flight, and static measurement of the synchro backlash (±0.43 m). The calculated result, ±1.87 m (Table 2a), is attributed to dynamic synchro backlash and includes some influence of short-term altitude variations. Long-period drift was examined by a 3.5 h laboratory test with a delay line to simulate a nonzero altitude. As shown in Table 2, these drifts are of the order of several meters. Also indicated is the change in output (±1.07 m) due to changes in signal strength.

From the above tests, the root-mean-square (rms) altimeter error for 4 h operation due to drift and signal variation is estimated to be ~0.5 m h^{-1}. At typical Sabreliner ground speeds of 200 m s^{-1},

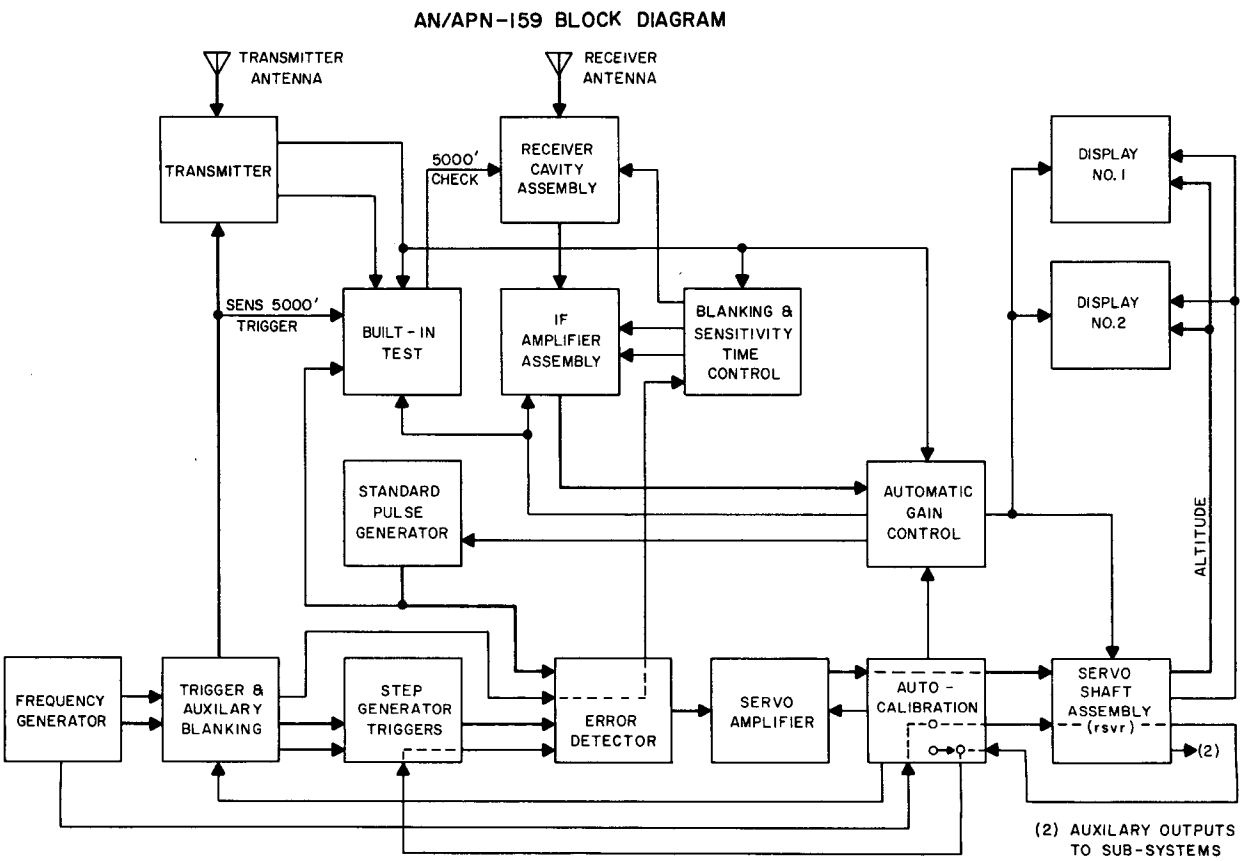

FIG. 1. Block diagram of altimeter set APN/159.

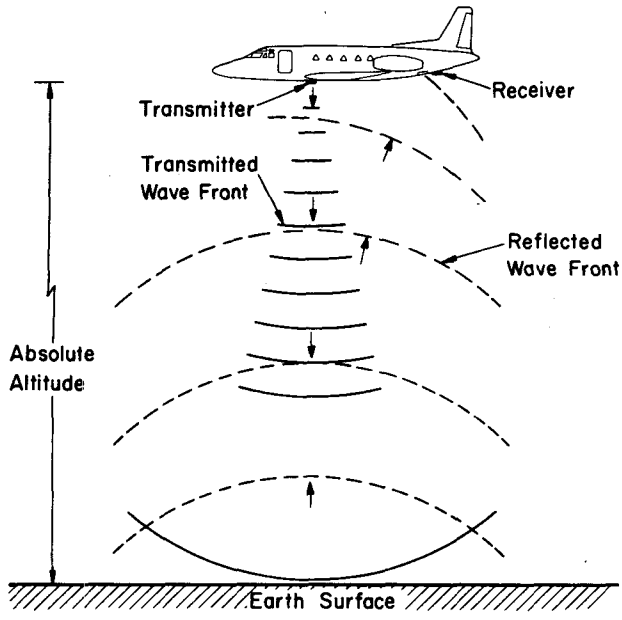

FIG. 2. Schematic of radar altimeter installation and transmitted/reflected wave fronts.

averaged height gradient changes $\Delta Z/\Delta N$ in excess of ± 0.7 parts in 10^6 are detectable, where Z is altitude and N is the ground coordinate along the flight track. Short-term variation is estimated to be ± 1.87 m and may be smoothed with data filtering.

To determine absolute accuracy and other performance features, a test (unpublished) of various high-altitude radar altimeters has been conducted by the U.S. Air Force. A laser target ranger which has a three standard deviation accuracy of ± 6.1 m was used as the standard for comparison during over-water flights. Table 3 lists the differences between an APN-203 radar altimeter and the laser ranger as well as standard deviations at each altitude. (The APN-203 is identical to the APN-159 except that it operates at a frequency of 4030 MHz rather than 1630 MHz.) A total of 781 altitude comparisons were made. The absolute error was found to be 5–10 m, with standard deviations of 2.7–6.4 m.

TABLE 2. Altimeter error analysis.

(a) Short-term signal variation (fine synchro backlash)		±1.87 m
(b) System drift (3 h 35 min lab test)		
1. Maximum fine synchro drift	±1.69 m	
2. Maximum fine synchro drift with weak-to-strong signal variations at 9000 m	±1.07 m	
3. Synchro conversion error (least significant bit)	+0.07 m	
Total rms drift error		±2.74 m

TABLE 3. APN-203 absolute accuracy relative to laser target ranger.

Altitude (m)	1524	3048	3658	5487	6402	7317	9146
Average error (m)	4.26	7.31	10.36	10.06	16.97	8.84	10.06
Standard deviation (m)	2.79	3.96	3.35	3.24	6.4	3.96	5.79
Percent error (%)	0.27	0.23	0.28	0.18	0.26	0.12	0.10

The lower limit of absolute accuracy is estimated to be ±11.1–16.1 m.

Gross radar altitude errors due to airplane pitch and roll displacement can be important. The antenna beam width of 45° provides a good margin of design safety for pitch and roll influences without stabilization. Aircraft maneuvers have suggested that roll in excess of the specified 18–20° introduces errors which cannot be corrected. However, the expected airplane rotation of ±6–8° during severe turbulence is not sufficient to downgrade system operations, as opposed to pilot-induced roll influences, which are easily detected.

The signal returned from scatters on a sea surface is complicated by a number of parameters, principally the depression angle (angle below the horizontal at which the sea is viewed), the radar polarization and frequency, and the condition of the sea surface. A full discussion of the sea surface scatters is beyond the scope of this analysis; researchers should consult the work of Katzin (1957), Grant and Yaplee (1957), and Moore and Williams (1957). It is sufficient to point out that the physical resolution element of the radar altimeter for a given set of operational conditions (range, beam widths) will vary with small depression angles and surface wind speed, but near vertical incidence this trend is reversed; at vertical incidence the radar area is not significantly altered by surface wind speed. The meteorological experiments reported in this paper were performed over oceanic areas and with controlled aircraft roll which held the angle of incidence near 90° during the data acquisition. Thus variations in the received signal due to the state of the sea are expected to be small.

3. Meteorological application

Measurements of the altitude above sea level of specified constant-pressure surfaces provide data for the basic meteorological analysis of winds. Routine wind soundings are taken globally twice a day from land-based sites using balloonborne sensors. Isobaric height observations are also obtained through remote sensing techniques from meteorological satellites. Though these observational methods are adequate to describe the large-scale (~1000 km) flow regimes of the atmosphere, they are unable

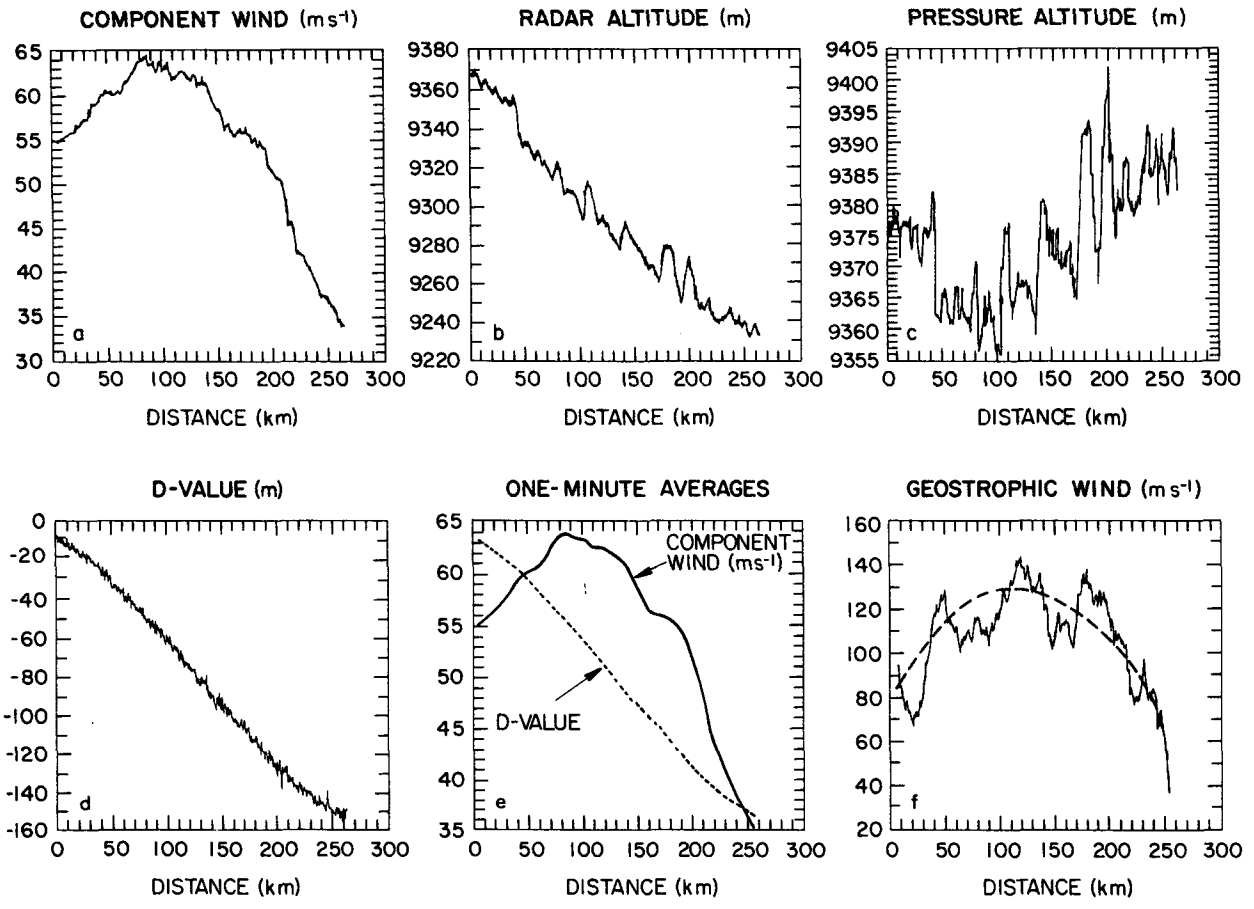

FIG. 3. From a 265 km Sabreliner flight segment on 1 March 1979 at 285 mb off the coast of California: (a) the observed wind component parallel to constant height contours, (b) radar altitude, (c) pressure altitude derived from the U.S. Standard Atmosphere, (d) D-value, equal to radar altitude minus pressure altitude, (e) 1 min averages of the component wind and D-value, (f) the computed geostrophic wind, with the dashed line showing a smoothed version.

to delineate the properties of the isobaric height fields on the small scale (~100 km) which are characteristic of the narrow jet stream currents found between 7 and 12 km altitude in middle and high latitudes. The problem arises from: 1) inaccuracies in heights derived from balloon soundings, which increase with altitude to over 60 m above 9 km; 2) poor spatial resolution of balloon soundings (~400 km separation between continental-based sounding stations); and 3) inherent inaccuracies in converting satellite radiation measurements of temperature into geometric heights of isobaric surfaces. An early work showing the usefulness of radar altimetry in meteorology is by Bellamy (1945), although no results with high spatial resolution were presented. The discussion that follows will illustrate the capability of radar altimeter technology in providing near-continuous spatial distributions of isobaric heights with an accuracy far surpassing that of balloon and satellite observing techniques.

In the meteorological application of radar altimetry, the parameter of interest is the D-value or difference between the absolute altitude Z_r and that indicated by the static pressure Z_p. In addition to

TABLE 4. Static pressure error estimate.

(a) Static source compensation ΔP*	±0.6 mb
(b) Static pressure transducer hysteresis, repeatability**	±0.1 mb
(c) Amplifier calibration stability ± 0.3 ppm full scale day^{-1}	±0.003 mb
(d) Primary standard uncertainty	±0.20 mb
(e) A-D converter error	±0.12 mb
rms static pressure error	0.65 mb

* Sabreliner static pressure correction developed from tower flyby calibration method: $\Delta P = -0.8017 + q_c(0.0301 + q_c 0.0001744)$, where q_c = dynamic pressure in mb.

** From short-term laboratory test, observing change in pressure transducer output resulting from ±2 mb change in input at a nominal pressure of ~300 mb.

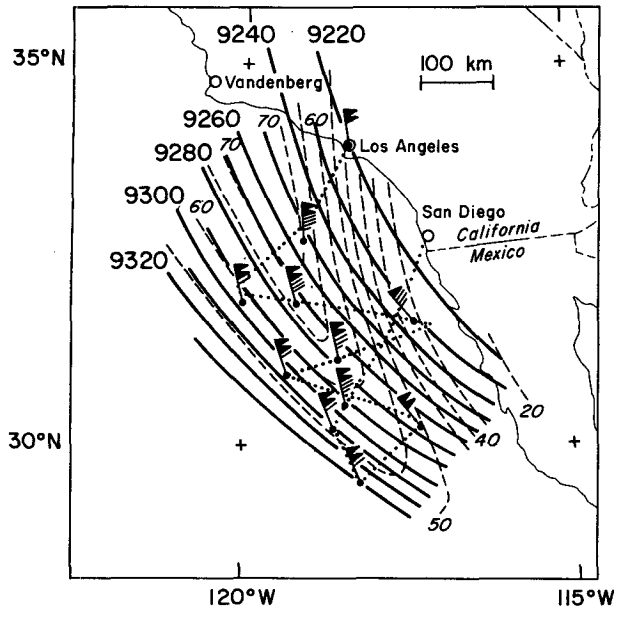

FIG. 4. Contours of adjusted radar altitude (m) (solid) and observed total wind (m s^{-1}) (dashed), from a Sabreliner flight on 1 March 1979 at 285 mb through strong cyclonic activity off the coast of southern California. The barbs show wind direction and speed with flag = 50 kt, full barb = 10 kt, half barb = 5 kt. The Sabreliner flight track is shown as a dotted line. The traces in Fig. 3 are from the nearly west–east leg in center.

errors in our radar-determined Z_r, there are pressure errors which contribute to uncertainties in D. The static pressure error analysis is presented in Table 4, which shows error sources of (a) static pressure correction due to flow field effects around the Sabreliner, (b) pressure transducer hysteresis, (c) electronic amplifier stability, (d) reference pressure standard stability, and (e) analog-to-digital conversion error. These amount to an rms static pressure error of 0.65 mb. The final rms-estimated error in D-value at 300 mb (9 km) altitude is ±6.0 m. This estimate assumes an rms pressure error of ±0.25 mb at 9 km; the static correction error, constant at constant speed, is not included.

To illustrate the application of radar altimetry, the results of a jet stream dynamics experiment which utilized the NCAR Sabreliner are presented here. Data for a well-developed jet stream from a flight off the coast of southern California on 1 March 1979 are compared to the actual wind measurement from the Sabreliner's pitot-static/inertial navigation wind system.

Fig. 3a shows the profile of the component of the measured horizontal wind speed V parallel to the height contours, versus the distance along the Sabreliner flight track; it illustrates a typical wind distribution across a narrow jet stream current near 9 km altitude. From Newton's second law of motion applied on the rotating earth, the wind speed is approximately proportional to the gradient of height measured perpendicular to the wind direction on an isobaric surface. The geostrophic wind speed V_g is given by

$$V_g = -\frac{g}{2\Omega \sin\phi}\frac{\partial Z}{\partial N}, \qquad (1)$$

where g is the acceleration of gravity, Ω the angular velocity of the earth, ϕ geographical latitude, Z the height of the pressure surface, and N the horizontal distance, normal to the left of the wind flow in the Northern Hemisphere. The expression $\partial Z/\partial N$ is the height gradient, i.e., the incremental change in height ΔZ in the distance ΔN. From Eq. (1), it is expected that the height of the pressure surface will decrease across the jet stream for a west-to-east traverse of the southward flowing jet stream.

The distribution of radar altitude (Z_r) versus distance for the jet stream traverse is presented in Fig. 3b. The expected decrease of Z_r is evident with a total height change of 130 m in the 265 km of the flight leg. The numerous fluctuations in the height profile are mostly due to the Sabreliner autopilot and to small-scale turbulent motions which vertically displace the aircraft from the nominal constant-pressure altitude surface on which it is attempting to fly. This is evident from Fig. 3c, which shows the Sabreliner pressure altitude (Z_p) trace within which are found both large- and small-scale fluctuations of up to 30 m. Z_p is determined from the assumption of a standard atmosphere. The fluctuations in Z_p may be removed by calculating the D-value:

$$D = Z_r - Z_p. \qquad (2)$$

The D-value curve shown in Fig. 3d contains the height slope information and the high-frequency oscillations (period < 30 s) which were discussed in Section 2. These fluctuations were removed from the data with a 1 min running average filter, which when applied to the raw data of Figs. 3a and 3d yielded the data shown in Fig. 3e.

The data in Figs. 3a–3e depict a flight segment through a cyclonically curved jet stream where the geostrophic wind can differ appreciably from the observed wind. The calculated geostrophic wind (Fig. 3f) is larger than the measured wind, but the general shape of the trace, shown as a dashed line, compares well with the observed wind. The ~50 km scale "waves" in Fig. 3f are probably real, and might be due to unsteady travelling pressure oscillations.

From Section 2, the error in D-value was estimated to be ± 6.0 m which corresponds to an uncertainty in the geostrophic wind of $\pm 5\%$ for the present data. In this example, the geostrophic wind was large, and easily measurable above aircraft system noise and accuracy limitations.

The height distribution of the 285 mb pressure surface for the flight is shown in Fig. 4. The height analysis shown was derived solely from the Sabreliner radar altitude and pressure data. The measured wind data show the observed wind blowing at substantial angles to the geostrophic wind. The accuracy of these height line positions greatly surpasses that which is obtainable from conventional balloon- and satellite-derived height analyses.

Acknowledgments. We are grateful to Mr. Sam Shoenhals of the Naval Weapons Center, China Lake, California, for providing a long-term loan of the APN-159 hardware. Also, we thank Dr. Donald Lenschow of the National Center for Atmospheric Research for his helpful comments during the preparation of the manuscript.

REFERENCES

Bellamy, J. C., 1945: The use of pressure altitude and altimeter corrections in meteorology. *J. Meteor.*, **2**, 1–79.

Duncan, T. M., and R. C. Brown, 1978: A data acquisition system for airborne meteorological research. *Bull. Amer. Meteor. Soc.*, **59**, 1128–1134.

Grant, C. R., and B. S. Yaplee, 1957: Back scattering from water and land at centimeter and millimeter wavelengths. *Proc. IRE*, **45**, 976–982.

Katzin, M., 1957: On the mechanisms of radar sea clutter. *Proc. IRE*, **45**, 44–54.

Moore, R. K., and C. S. Williams, Jr., 1957: Radar terrain return at near-vertical incidence. *Proc. IRE*, **45**, 228–238.